International Journal of Nanomedicine

Dovepress
open access to scientific and medical research

Open Access Full Text Article

ORIGINAL RESEARCH

Synthesis and antitumor activity of novel pyridinium fullerene derivatives

This article was published in the following Dove Press journal:
International Journal of Nanomedicine

Takumi Yasuno[1]
Tomoyuki Ohe[1]
Hitomi Ikeda[1]
Kyoko Takahashi[1]
Shigeo Nakamura[2]
Tadahiko Mashino[1]

[1]Department of Pharmaceutical Sciences, Faculty of Pharmacy, Keio University, Tokyo, Japan; [2]Department of Chemistry, Nippon Medical School, Tokyo, Japan

Purpose: We have previously reported that some cationic fullerene derivatives exhibited anticancer activity, and they are expected to be a potential lead compound for an anti-drug resistant cancer agent. However, they are bis-adducts and a mixture of multiple regioisomers, which cannot be readily separated due to the variability of substituent positions on the fullerene cage. To overcome this issue, we evaluated the antiproliferative activities of a set of mono-adduct derivatives and examined their structure-activity relationship. In addition, the in vivo antitumor activity of selected derivatives was also examined.

Methods: Nineteen pyridinium fullerene derivatives were newly designed and synthesized in this study. Their antiproliferative activities were evaluated using several cancer cell lines including drug-resistant cells. Furthermore, in vivo antitumor activity of several derivatives was investigated in mouse xenograft model of human lung cancer.

Results: The derivatives inhibited the proliferation of cancer cell lines, including cisplatin-resistant cells and doxorubicin-resistant cells. It was also shown that compound **10** (10 μM), **13** (10 μM) and *cis*-**14** (10 μM) induced the intracellular oxidative stress. In addition, compound **13** (20 mg/kg) and *cis*-**14** (15 mg/kg) significantly exhibited antitumor activity in mouse xenograft model of human lung cancer.

Conclusion: We synthesized a novel set of mono-adduct fullerene derivatives functionalized with pyridinium groups and found that most of them show potent antiproliferative activities against cancer cell lines and some of them show significant antitumor activities in vivo. We propose that these fullerene derivatives serve as the lead compounds for a novel type of antitumor agents.

Keywords: fullerene, anticancer agents, cisplatin-resistant cancer, doxorubicin-resistant cancer, P-glycoprotein

Introduction

Cancer is the second leading cause of human mortality and it is estimated that there will be over ten million deaths from cancer up to 2030 worldwide.[1] While chemotherapy treats many types of cancer effectively, chemotherapy fails in over 90% of metastatic cancer patients due to multidrug resistance (MDR).[2] A variety of MDR mechanisms have been characterized. Alteration in target proteins, drug metabolism, cellular repair mechanisms, and drug efflux pumps, such as P-glycoprotein (P-gp), can give rise to anticancer drug resistance.[3] Once tumors acquire MDR, they become resistant to many anticancer drugs at the same time. Therefore, there is an urgent need for a new class of drugs for cancer treatment.

Fullerene, discovered in 1985, is a carbon allotrope and is expected to be pharmaceutically useful due to its molecular structure.[4,5] However, evaluation of

Correspondence: Tomoyuki Ohe; Tadahiko Mashino
Department of Pharmaceutical Sciences, Faculty of Pharmacy, Keio University, 1-5-30 Shibakoen, Minato-ku, Tokyo, Japan
Tel +81 35 400 2691; +81 35 400 2694
Fax +81 35 400 2691
Email ohe-tm@pha.keio.ac.jp; mashino-td@pha.keio.ac.jp

submit your manuscript | www.dovepress.com
DovePress
http://doi.org/10.2147/IJN.S212045

the potency of fullerene has been limited by its high hydrophobicity. To overcome this issue, various types of fullerene derivatives with hydrophilic substituents have been studied. Water-soluble fullerene derivatives are reported to possess a range of pharmacological properties, including inhibitory effects against various enzymes such as cysteinic/serinic protease, HIV protease, HCV NS3/4A protease, HCV NS5B polymerase, and HIV reverse transcriptase, as well as antibacterial and antiproliferative activities.[6–14]

We have previously reported that C_{60}-bis(*N,N*-dimethylpyrrolidinium iodide) (**1**) (Figure 1) and its analogues exhibited anticancer activity by increasing intracellular oxidative stress and inducing apoptosis.[15] In addition, the study using cancer cell line panels which enable evaluation of the antiproliferative activities of a compound in 39 human cancer cell lines suggested that **1** and its analogues are unique anticancer agents with a novel mechanism of action that is different from the mechanisms of existing anticancer drugs such as bleomycin, cisplatin, doxorubicin, etoposide, 5-fluorouracil, paclitaxel, tamoxifen, topotecan, and vincristine.[16] Thus, **1** is expected to be a potential lead compound for an anti-drug resistant cancer agent. However, **1** is a bis-adduct and a mixture of multiple regioisomers, which cannot be readily separated due to the variability of substituent positions on the fullerene cage.

To overcome this issue, we evaluated the antiproliferative activities of a set of mono-adduct derivatives (**2**–*trans*-**19**) containing dication functionalized with pyridinium groups using drug-resistant cancer cell lines and examined their structure-activity relationship (SAR) in the present study (Figure 1). Furthermore, the in vivo antitumor activity of several derivatives was investigated in mouse xenograft model of human lung cancer.

Materials and methods

General

^{1}H-NMR spectra were measured using a Varian 400 or 500 FT-NMR instrument operating at 400 and 500 MHz, respectively, with tetramethylsilane as an internal standard (δ=0.00) in $CDCl_3$ or DMSO-d_6. MALDI-TOF-MS spectra were recorded using a Shimadzu AXIMA-CFE Plus instrument. ESI-TOF-MS spectra were recorded using a JEOL JMS-T100LP instrument. Luminescence was measured using Tecan M200. Column chromatography was performed using a Merck Silica gel 60. C_{60} (99.95+%) was purchased from MTR Ltd. Dimethyl sulfoxide was purchased from Aldrich chemical Co. K562 and K562/ADM were provided by National Institutes of Biomedical Innovation, Health and Nutrition. NIH:OVACR-3 was provided by ATCC. A549, HepG2 and HeLa was provided by the RIKEN BRC through the National Bio-Resource Project of the MEXT, Japan. RPMI-1640 medium, DMEM medium (low glucose) and the penicillin-streptomycin solution were purchased from Sigma Inc. Heart-inactivated fatal bovine serum was purchased from Life Technologies Co. MEM medium, MEM NEAA and DMEM medium (high glucose,

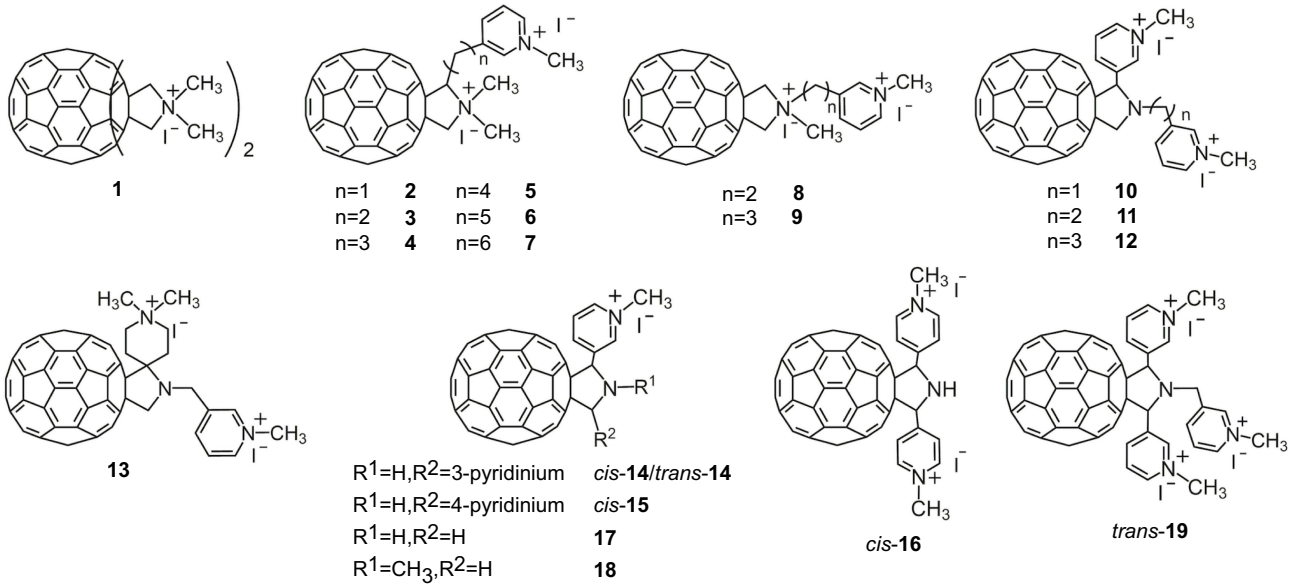

Figure 1 Structures of fullerene derivatives.

HEPES, no phenol red) were purchased form ThermoFisher Scientific. Other chemicals used were of the highest quality commercially available.

Synthesis of fullerene derivatives

The precursors (**2′-18′**) of all fullerene derivatives were synthesized via 1,3-dipolar cycloaddition of azomethine ylides, generated from glycine analogues or 3/4-picolylamine derivatives and various aldehydes. In the case of **2′-13′, 17′** and **18′**, corresponding azomethine ylides were formed along with decarboxylation in situ.

Briefly, derivatives **2**–**7** were synthesized by 1,3-dipolar cycloaddition reaction of sarcosine and ω-(3-pyridyl) alkanal, which were generated by Dess-Martin oxidation of corresponding alcohols, onto C_{60}, followed by methylation of **2′-7′** with methyl iodide (Scheme 1).

Derivatives **8**–**13** were synthesized by 1,3-dipolar cycloaddition reaction of *N*-(3-pyridylalkyl)glycine and paraformaldehyde, 3-pyridinecarboxaldehyde or *N*-methyl 4-piperidone followed by the methylation of **8′-13′** with methyl iodide (Scheme 2).

Derivatives *cis*-**14**–**18** were synthesized in a similar manner to **2**–**7** (Scheme 3). The introduction of the methyl groups onto the pyridine nitrogen was confirmed by the downfield shift of the ^{1}H NMR signals for the aromatic protons in *cis*-**14**–**18** and the observation of an NH resonance in *cis*-**14**–**17**. In the case of **10**–**18**, a pyrrolidine ring amino moiety was not methylated due to the steric hindrance and low nucleophilicity.

The synthetic details and analytical data of all the derivatives are available in supplementary materials.

We have previously reported that the formation of the *cis* isomer may be explained by a mechanistic hypothesis in which the (*E, E*) azomethine ylide intermediate (which leads to the *cis* product) generated from the corresponding primary amine and ketone or aldehyde is more dominant than the other configurations due to its steric stability. In contrast, in the case of a secondary amine, (*E, Z*) or (*Z, E*) azomethine ylide, which produces a *trans* isomer, would be generated predominantly due to the steric stability.[8] On the basis of this finding, derivatives *trans*-**14** and *trans*-**19** were synthesized by the 1,3-dipolar cycloaddition reaction of 3-pyridinecarboxaldehyde and *N*-(4-methoxybenzyl)-3-picolylamine or bis(3-picolyl)amine, respectively, followed by methylation with methyl iodide (Scheme 4). In fact, the methine proton on C-5 of the pyrrolidine ring in the *trans* isomers was obviously downfield-shifted compared to the *cis* isomer, which was consistent with the report by Filippone et al.[17]

Cell culture

HL60 cells were cultured in the RPMI-1640 medium supplemented with 5% heart-inactivated fatal bovine serum,

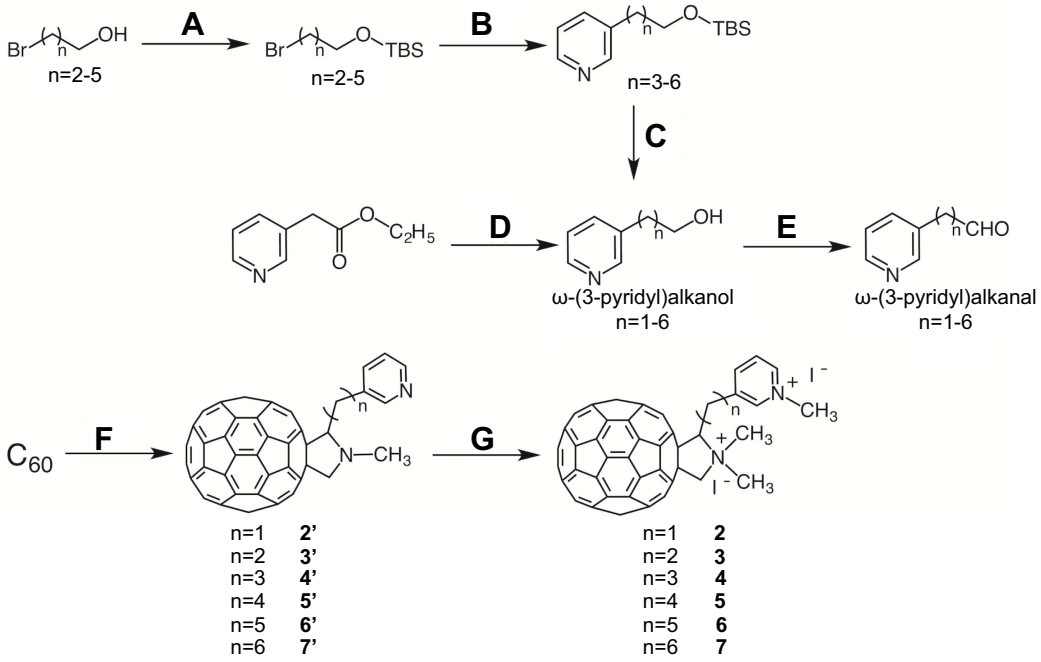

Scheme 1 Synthesis of **2**–**7**. (**A**) TBS chloride, imidazole, THF, r.t; (**B**) 3-methylpyridine, LDA, THF, −78 °C to r.t; (**C**) TBAF, THF, r.t, 50–87% (in three steps); (**D**) $LiAlH_4$, THF, r.t, quant; (**E**) DMP, CH_2Cl_2, r.t, 25–64%; (**F**) ω-(3-pyridyl)alkanal, sarcosine, toluene, reflux, 30–38%; (**G**) methyl iodide, r.t, 54–100%.
Abbreviations: TBS, tert-butyldimethylsilyl; THF, tetrahydrofuran; LDA, lithium diisopropylamide; TBAF, tetrabutylammonium fluoride; DMP, Dess-Martin periodionane.

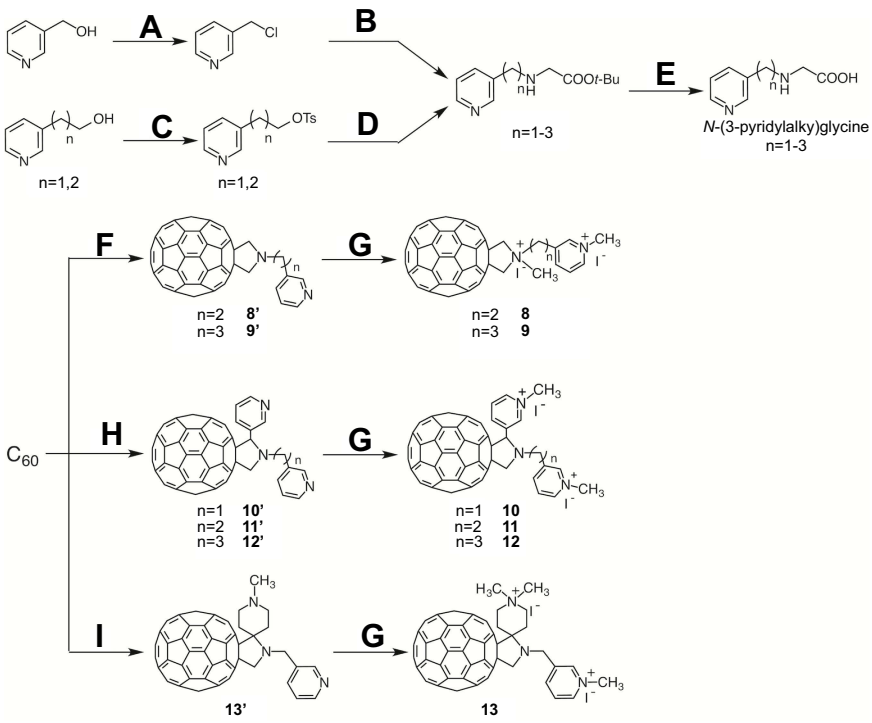

Scheme 2 Synthesis of **8**–**13**. (**A**) thionyl chloride, CH_2Cl_2, reflux, quant; (**B**) glycine *tert*-butyl ester hydrochloride, triethylamine, ethanol, reflux, 59%; (**C**) tosyl chloride, KOH, THF, r.t, 96–100%; (**D**) glycine *tert*-butyl ester hydrochloride, $NaHCO_3$, acetonitrile, 60 °C, 22–37%; (**E**) TFA, toluene, r.t, quant; (**F**) paraformaldehyde, *N*-(3-pyridylalkyl)glycine, DIEA, toluene, reflux, 11–33%; (**G**) methyl iodide, r.t, 85–92%; (**H**) 3-pyridinecarboxaldehyde, *N*-(3-pyridylalkyl)glycine, DIEA, toluene, reflux, 12–34%; (**I**) *N*-methyl-4-piperidone, *N*-(3-pyridylalkyl)glycine, DIEA, toluene, reflux, 21%.

Abbreviations: THF, tetrahydrofuran; DIEA, *N*,*N*-diisopropylethylamine.

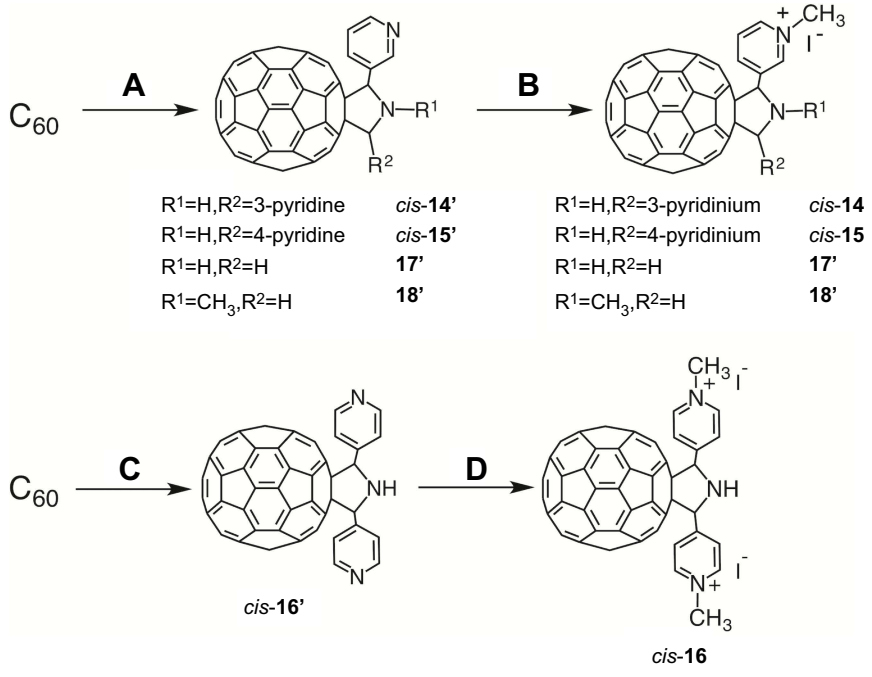

Scheme 3 Synthesis of *cis*-**14**–**18**. (**A**) 3-pyridinecarboxaldehyde, 3/4-picolylamine or glycine derivative, *o*-dichlorobenzene or toluene, reflux, 13–32%; (**B**) methyl iodide, r.t, 24–81%; (**C**) 4-pyridinecarboxaldehyde, 4-picolylamine, *o*-dichlorobenzene, reflux, 26%;(**D**)methyl iodide, r.t, 88%.

100 IU/mL penicillin and 100 mg/mL streptomycin at 37 °C in a 5% CO_2 incubator with a humidified atmosphere. A549 cells were cultured in the DMEM medium (low glucose) supplemented with 10% heart-inactivated fatal bovine serum, 100 IU/mL penicillin and 100 mg/mL streptomycin at 37 °C in a 5% CO_2 incubator with a humidified

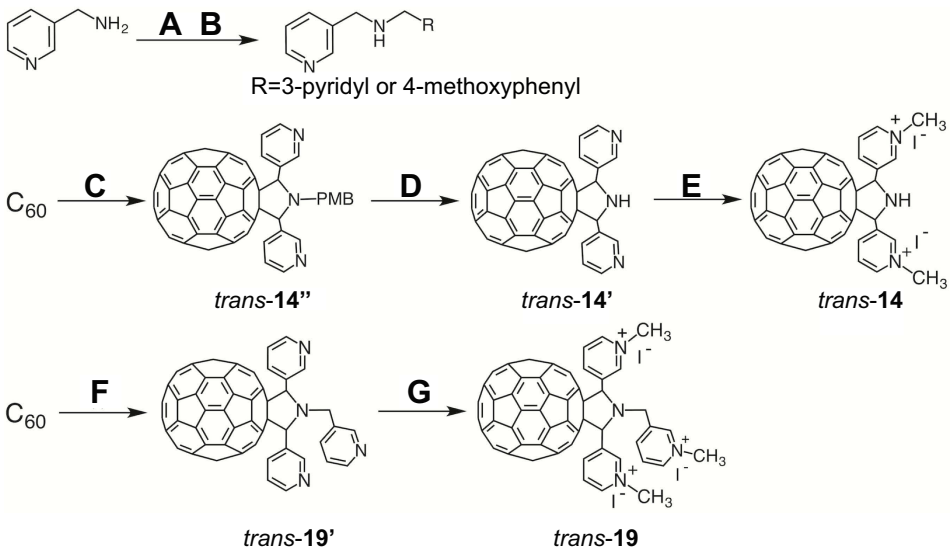

Scheme 4 Synthesis of *trans*-**14**, *trans*-**19**. (**A**) 3-pyridinecarboxaldehyde or 4-methoxybenzylaldehyde, methanol, r.t; (**B**) sodium borohydride, r.t, 86–92% (in two steps); (**C**) 3-pyridinecarboxaldehyde, 3-(*N*-4-methoxybenzyl)picolylamine, *o*-dichlorobenzene, reflux, 6.2%; (**D**) TFA, chloroform, r.t, quant; (**E**) methyl iodide, r.t, 62%; (**F**) 3-pyridinecarboxaldehyde, bis(3-picolylamine), acetic acid, toluene, reflux, 32%; (**G**)methyl iodide, r.t, 93%.

atmosphere. HepG2 cells were cultured in the MEM medium supplemented with 10% heart-inactivated fatal bovine serum, 100 IU/mL penicillin and 100 mg/mL streptomycin at 37 °C in a 5% CO_2 incubator with a humidified atmosphere. HeLa cells were cultured in the MEM (1x) medium supplemented with 10% heart-inactivated fatal bovine serum, 1% MEM NEAA (100x), 100 IU/mL penicillin and 100 mg/mL streptomycin at 37 °C in a 5% CO_2 incubator with a humidified atmosphere. NIH:OVCAR-3 and K562 cells were cultured in the RPMI-1640 medium supplemented with 10% heart-inactivated fatal bovine serum, 100 IU/mL penicillin and 100 mg/mL streptomycin at 37 °C in a 5% CO_2 incubator with a humidified atmosphere. K562/ADM cells were cultured in the RPMI-1640 medium supplemented with 10% heart-inactivated fatal bovine serum, 100 IU/mL penicillin, 100 mg/mL streptomycin and 300 ng/mL adriamycin at 37 °C in a 5% CO_2 incubator with a humidified atmosphere. NIH3T3 cells were cultured in the DMEM medium (high glucose, HEPES, no phenol red) supplemented with 10% heart-inactivated fatal bovine serum, 100 IU/mL penicillin and 100 mg/mL streptomycin at 37 °C in a 5% CO_2 incubator with a humidified atmosphere.

Antiproliferative assay and cytotoxicity assay

Cancer cells were seeded in six-well multi-plates (2.0×10^5 cells/well), and the test compounds in DMSO (final concentration of DMSO was 0.5 v/v%) were added followed by incubation for 24 h at 37 °C under 5% CO_2 atmosphere. After incubation, the cells were collected and centrifuged at 100 G for 5 min. The medium was replaced by the same volume of the phosphate buffered saline (-), and the cells were re-suspended. The suspension was mixed with the trypan blue dye and viable cells were counted by the dye exclusion method using a Vi-CELL^{TM} XR instrument (Beckman Counter Inc.). The cell viability was expressed relative to the vehicle control (DMSO only) group (n=3).

Effect of α-tocopherol on fullerene derivatives-induced cell death in HL60

HL60 cells were seeded in six-well multi-plates (2.0×10^5 cells/well), and pre-incubated with α-tocopherol for 3 h at 37 °C under 5% CO_2 atmosphere. Then, the cells were treated with the test compounds in DMSO (final concentration of DMSO was 0.5 v/v%) for 24 h 37 °C under 5% CO_2 atmosphere. After incubation, the cells were collected and centrifuged at 100 G for 5 min. The medium was replaced by the same volume of the phosphate buffered saline (-) and the cells were re-suspended. The suspension was mixed with the trypan blue dye and viable cells were counted by the dye exclusion method using a Vi-CELL^{TM} XR instrument (Beckman Counter Inc.). The cell viability was expressed relative to the vehicle control (DMSO only) group (n=3).

Measurement of intracellular oxidative stress

HL60 cells were seeded in six-well multi-plates (5.0×10^5 cells/well) and treated with 2',7'-dichlorodihydrofluorescein diacetate (DCFH-DA) (10 μM) for 15 min at 37 °C under 5% CO_2 atmosphere. After pre-incubation, the cells were washed with phosphate buffered saline (-) and medium was exchanged. The cells were re-seeded with the test compounds in DMSO (final concentration of DMSO was 0.5 v/v%) for 1.0 h at 37 °C under 5% CO_2 atmosphere. After incubation, cells were collected and centrifugated at 100 G for 5 min. The pellet was re-suspended in 1 mL of BD FACS flow™ (BD, Japan) and cellular-fluorescence was quantified using a BD FACSCalibur™ flow cytometer (BD, Japan) with excitation and emission settings of 488 and 530 nm, respectively. FACS analysis was performed with about 10,000 cells for each sample. The obtained data were analyzed by BD CellQuest™ Pro.

Condensation of nuclear chromatin

HL60 cells were seeded in six-well multi-plates (5.0×10^5 cells/well), and the test compounds in DMSO (final concentration of DMSO was 0.5 v/v%) were added followed by incubation for 24 h at 37 °C under 5% CO_2 atmosphere. After incubation, the cells were fixed in 1.0% glutaraldehyde for 30 min at room temperature. After washing with the phosphate buffered saline (-), cells were stained with Hoechst 33342 (167 μM) and observed using fluorescence microscopy.

Activation of caspase-3/7

HL60 cells were seeded in six-well multi-plates (2.0×10^4 cells/well), and the test compounds in DMSO (final concentration of DMSO was 0.5 v/v%) were added followed by incubation for 24 h at 37 °C under 5% CO_2 atmosphere. After incubation, the activities of caspase-3/7 in cell lysates were measured using the Caspase-Glo assay kit according to the manufacturer's protocols (Promega, Madison, WI, USA). Luminescence was measured as relative light unit (RLU) on Tecan M200 and the caspase activities were expressed as a ratio to the mean value in untreated cells.

Effect of quinidine on fullerene derivatives-induced cell-death in K562/ADM

Cancer cells were seeded in six-well multi-plates (2.0×10^5 cells/well), and the test compounds or quinidine in DMSO (final concentration of DMSO was 1.0 v/v%) were added followed by incubation for 24 h at 37 °C under 5% CO_2 atmosphere. After incubation, the cells were collected and centrifuged at 100 G for 5 min. The medium was replaced by the same volume of the phosphate buffered saline (-) and the cells were re-suspended. The suspension was mixed with the trypan blue dye and viable cells were counted by the dye exclusion method using a Vi-CELL™ XR instrument (Beckman Counter Inc.). The cell viability was expressed relative to the vehicle control (DMSO only) group (n=3).

In vivo antitumor experiment

Four-week-old female BALB/c nude mice were purchased from Sankyo Labo Service corporation, Inc. The animals had free access to a commercial diet and water in animal cages under a pathogen-free condition at 25±1 °C and humidity of 45±10% in a 12 h dark and light cycles.

In order to test the antitumor activity of fullerene derivatives in vivo, A549 cells (1.0×10^7 cells) were injected subcutaneously into female BALB/c nude mice aged 4 weeks. After injection of A549 cells, the mice were treated daily for 6 days with an intraperitoneal injection of fullerene derivatives. The animals were sacrificed and the weights of the tumor, liver and spleen were recorded at two weeks after tumor cell inoculation (Day 20) (n=4).

Animal welfare and experimental procedures were performed strictly in accordance with the Care and Use of Laboratory Animals and approved by the Keio University Animal Research Committee (approval number: 17043). All efforts were made to minimize the animals' suffering and to reduce the number of animals used.

In vitro statistical analysis

All in vitro data are presented as mean ± SD of at least three independent experiments. Statistical difference were evaluated using the Student's *t*-test at significance levels of $p<0.05$.

In vivo statistical analysis

All in vivo data are presented as mean ± SD. Statistical analysis for group comparison was performed using one-way ANOVA with Dunnett's post hoc test by JMP version 13 at significance levels of $p<0.05$.

Results and discussion

Antiproliferative activities of fullerene derivatives for HL60

We first investigated the antiproliferative activities of the fullerene derivatives using human leukemia cells, HL60.

HL60 cells were exposed to fullerene derivatives for 24 hrs and cell viability was measured by the trypan blue exclusion assay (Table 1). With the exception of **2**, *cis*-**15**, *cis*-**16, 17** and **18**, the newly synthesized fullerene derivatives were more potent than **1**. The comparison among compounds **2**–**7**, bearing various alkyl spacers at the 2-position on the pyrrolidinium ring, suggested that a longer spacer is superior to a shorter one (**7**>**3, 4, 5, 6**>**2**). In addition, **8** and **9** showed less activity than **3** and **4**, respectively, suggesting that the introduction of a pyridinium moiety onto the 2-position on the pyrrolidinium ring is more preferable than the introduction onto the 1-position. Furthermore, **10**–**12**, *cis*/*trans*-**14** and *trans*-**19** which have two or three 3-pyridinium moieties, inhibited the HL60 growth more strongly than **2**–**9** which have a single 3-pyridinium moiety in addition to a pyrrolidinium cation, while there was no difference in the activity among **10**–**12**, *cis/trans*-**14** and *trans*-**19**. These results suggested that a 3-pyridinium is more desirable for strong antiproliferative activity than a pyrrolidinium and that the steric positions of the two pyridinium groups in the molecule may not be important. On the other hand, *cis*-**15** and *cis*-**16** lack the antiproliferative activity, clearly indicating that 4-pyridinium cannot be substituted for 3-pyridinium. Moreover, **17** and **18** lack the antiproliferative activity, indicating that one cationic group is undesirable. The activity of **13** which contains a spiro piperidinium and a 3-pyridinium in the molecule is comparable to the activities of the derivatives containing multiple 3-pyridinium moieties, suggesting that 3-pyridinium on the pyrrolidine ring can be replaced by spiro piperidinium.

Table 1 Antiproliferative activity of fullerene derivatives for HL60 cells

Compound	HL60 growth inhibition IC_{50} (μM)
1	32.2
2	>50
3	10.1
4	11.6
5	9.0
6	9.5
7	6.1
8	28.4
9	17.1
10	3.6
11	6.6
12	3.1
13	3.2
cis-**14**	3.8
trans-**14**	3.5
cis-**15**	>50
cis-**16**	>50
17	>50
18	>50
trans-**19**	2.9
Cisplatin	2.7
Etoposide	1.4
Doxorubicin(ADM)	0.057

Apoptosis induction effects of fullerene derivatives

We have previously reported that fullerene derivative **1** induced apoptosis involving the generation of the reactive oxygen species (ROS) in HL60.[15] Accordingly, we examined the condensation of nuclear chromatin (Figure 2) and the activation of caspase-3/7 (Figure 3). The data clearly show that the condensation of nuclear chromatin was observed and caspase was activated after 24 hrs of the treatment with **10, 13** and *cis*-**14**. These results indicate that the fullerene derivatives induce apoptosis involved in caspase cascade in HL60 cells. Moreover, we examined the effect of α-tocopherol, an effective antioxidant, on the antiproliferative activities of the fullerene derivatives synthesized in the present study. Pre-treatment with α-tocopherol completely suppressed the fullerene derivatives-induced cell death (Figure 4). Fluorescent analysis of ROS using DCFH-DA demonstrated that **10, 13** and *cis*-**14** induce the intracellular oxidative stress (Figure 5). In particular, the DCF fluorescence intensity of the cells treated with both *cis*-**14** and α-tocopherol were weaker than that treated with only *cis*-**14** (Figure 6). These results suggest that the new fullerene derivatives induce apoptosis in HL60 cells mediated by ROS in the same way as **1**.

Antiproliferative activities for cancer cell lines and cytotoxicity for NIH3T3 of fullerene derivatives

Next, the antiproliferative activities of the fullerene derivatives that inhibited HL60 growth were examined for the A549, HepG2, HeLa, K562 and two-resistant cell lines, namely, NIH:OVCAR-3 (cisplatin-resistant) and K562/ADM (doxorubicin-resistant) (Table 2). The fullerene derivatives inhibited the proliferation of all cell lines tested with the similar structure-activity relationship to that observed in HL60. Especially, **10**, *cis*-**14** and *trans*-**19**, containing two 3-pyridinium moieties, were more potent to HepG2 than other fullerene derivatives. On the contrary, **11, 12** and *trans*-**14** showed less potency than **10**, *cis*-**14**

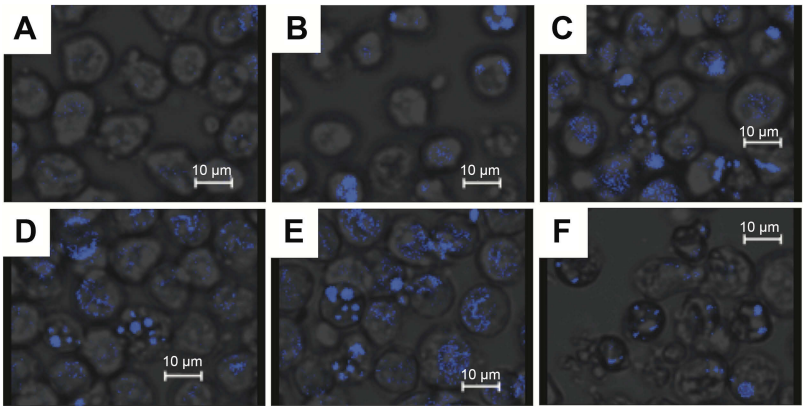

Figure 2 Morphological analysis of nuclear chromatin condensation after exposure of HL60 cells to fullerene derivatives. Cells were treated with fullerene derivatives and were stained with Hoechst 33342 (167 μM) ((**A**) Control, (**B**) **1** (32.5 μM), (**C**) **10** (5.0 μM), (**D**) **13** (5.0 μM), (**E**) *cis*-**14** (5.0 μM), (**F**) Doxorubicin (0.50 μM)).

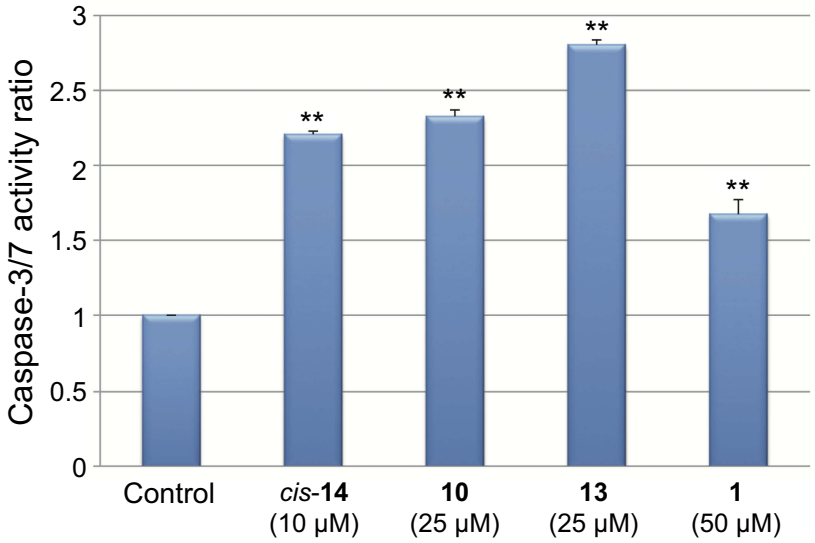

Figure 3 Activation of caspase-3/7 after exposure of HL60 cells to fullerene derivatives. Cells were treated with fullerene derivatives for 24 hrs followed by the addition of Caspase-Glo assay kit. **p<0.01 vs control.

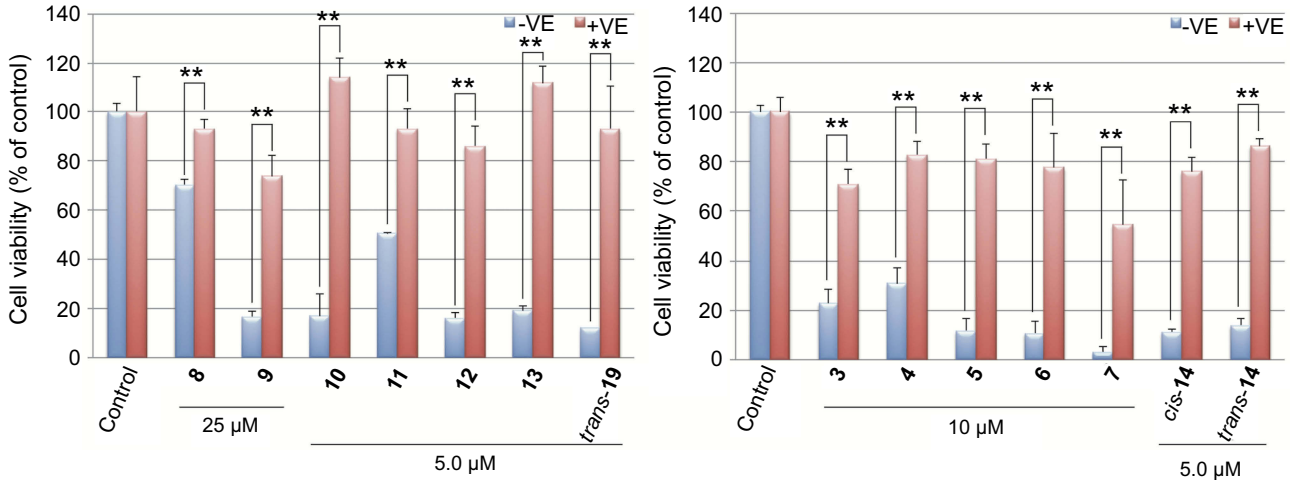

Figure 4 Effects of α-tocopherol on fullerene derivatives-induced cell death in HL60 cells. Cells were pre-incubated with α-tocopherol (300 μM) for 3 hrs prior to exposure to fullerene derivatives for 24 hrs. **p<0.01.

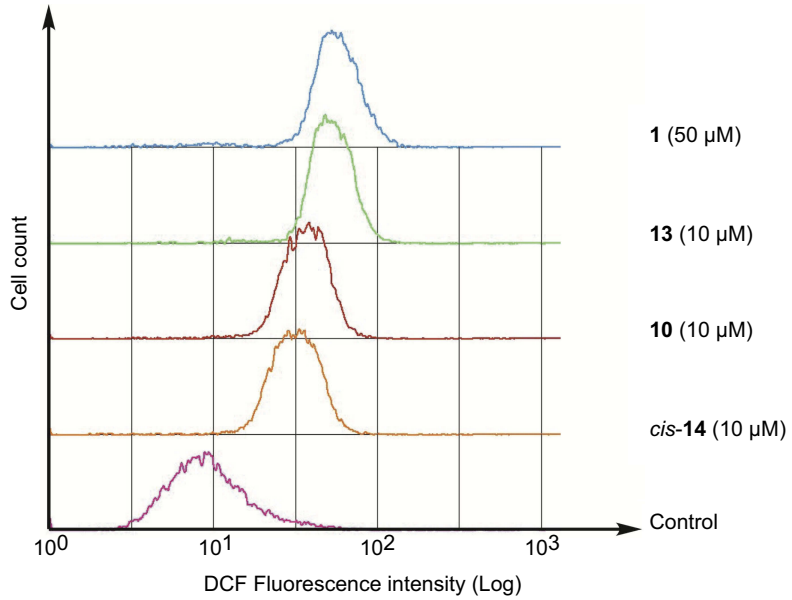

Figure 5 Intracellular oxidative stress in HL60 cells. Cells were pre-incubated with DCFH-DA (10 μM) for 15 min. Then, the cells were washed with phosphate buffered saline, followed by incubation with the fullerene derivatives for 1 hr. The cellular fluorescence was measured at 530 nm with excitation at 488 nm.
Abbreviation: DCFH-DA, 2',7'-dichlorodihydrofluorescein diacetate.

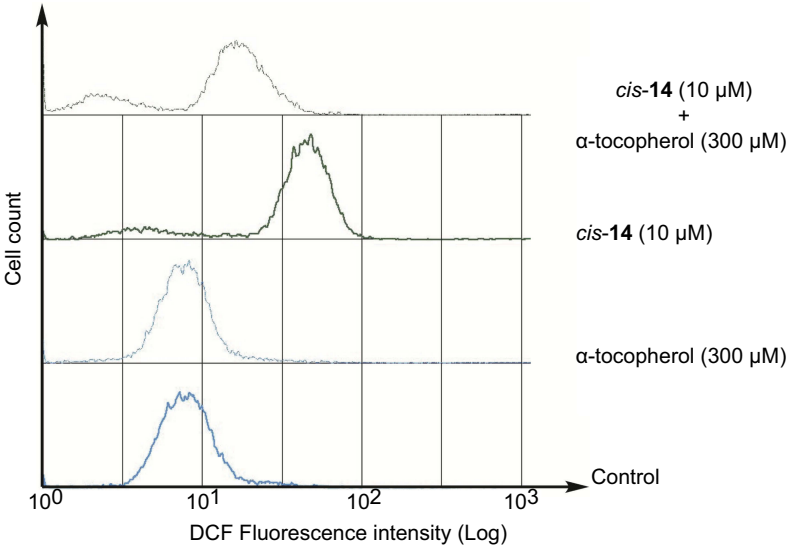

Figure 6 Effects of α-tocopherol on intracellular oxidative stress in HL60 cells treated *cis*-**14**. Cells were pre-incubated with α-tocopherol (300 μM) for 1 hr prior to exposure to fullerene derivatives for 1 hr. Oxidative stress was measured by DCFH-DA fluorescence probes.
Abbreviation: DCFH-DA, 2',7'-dichlorodihydrofluorescein diacetate.

and *trans*-**19**. These results suggest that the deposition of pyridinium moieties is important to demonstrate high antiproliferative activity to HepG2.

It should also be emphasized that all newly synthesized compounds shown in Table 2 were potent to NIH:OVCAR-3, as well as HeLa. This is the first report demonstrating antiproliferative activity of fullerene derivatives against drug-resistant cancer cell lines. In addition, these fullerene derivatives were shown to be more potent to K562/ADM with overexpressed of P-glycoprotein (P-gp) than doxorubicin, while the antiproliferative activities of some fullerene derivatives, eg, **7** and **10**, for K562/ADM were slightly lower than those for K562.

To evaluate the cytotoxicity of fullerene derivatives to non-cancerous normal cells, we examined cell viability after incubation with the derivatives in mouse fibroblast NIH3T3 cells (Table 2). The IC_{50} values for NIH3T3 were comparable to those for cancer cell lines, suggesting that

Table 2 Antiproliferative activity for cancer cell lines (HepG2, A549, HeLa, NIH:OVCAR-3, K562 and K562/ADM) and cytotoxicity for NIH3T3 of fullerene derivatives

Compound	Cell growth inhibition IC_{50} (μM)						
	NIH3T3	HepG2	A549	HeLa	NIH:OVCAR-3	K562	K562/ADM
1	>50	34.0	>50	31.2	28.4	21.1	22.1
3	21.3	7.3	12.0	16.1	9.9	11.3	14.4
4	12.2	10.4	16.2	13.0	11.3	11.4	16.8
5	5.8	7.4	13.1	11.1	10.4	10.8	13.7
6	6.0	5.2	12.6	10.7	10.9	9.4	15.2
7	4.2	5.8	7.1	7.3	8.6	5.4	11.8
10	4.6	0.014	5.7	6.2	7.6	4.2	8.9
11	11.5	6.9	7.0	6.9	6.4	8.9	10.7
12	4.9	4.5	5.1	5.0	7.1	4.9	8.6
13	6.6	4.0	7.4	6.7	7.6	5.4	9.9
cis-**14**	5.0	0.013	6.4	7.0	8.4	4.6	5.8
trans-**14**	6.0	5.1	9.4	7.5	9.5	4.5	6.7
trans-**19**	4.8	0.017	8.8	8.3	10.0	4.6	7.5
Cisplatin	N. T.	N. T.	N. T.	17.3	>100	N. T.	N. T.
Etoposide	1.5	14.0	N. T.	N. T.	N. T.	N. T.	N. T.
Doxorubicin(ADM)	N. T.	N. T.	0.20	N. T.	N. T.	0.14	15.8

Abbreviation: N.T, Not Tested.

in vitro cytotoxicity of fullerene derivatives was not low in normal cells. Therefore, as described later, we further investigated acute and sub-chronic toxicity in vivo.

Effect of quinidine on fullerene derivatives-induced cell-death in K562/ADM

Additional studies revealed that the antiproliferative activities of **7** (10 μM) and **10** (10 μM) in K562/ADM cells were significantly enhanced by the addition of a P-gp inhibitor, quinidine (Figure 7). In the case of *cis*-**14**, the enhancement of the antiproliferative activity was confirmed when a lower concentration of *cis*-**14** (7.5 μM) was co-incubated with quinidine. These results suggest that **7** and **10** and *cis*-**14** are substrates of P-gp and are extruded out of the cells by the transporter. It should be stressed that this is the first report showing functionalized fullerene derivatives can be substrates for P-gp.

In vivo antitumor activities of 10, 13 and cis-14 in mouse xenograft model

The antitumor effect of fullerene derivatives in vivo was investigated using a mouse xenograft model. Nude mice were subcutaneously injected with human lung cancer A549 cells and then treated with intraperitoneal injection of **10, 13**, *cis*-**14** or **1** for 6 days. The nude mice treated with fullerene derivatives exhibited no obvious alteration, including the weight of livers and spleens (Figure 8), suggesting that **10, 13**, *cis*-**14** and **1** showed low toxicity in vivo unlike their non-negligible cytotoxicity in vitro. Moreover, compared with control, the time-dependent growth of tumor volume was suppressed by administration of fullerene derivatives (Figure 9). Especially, the administration of **13** and **1** significantly reduced tumor volume and weight (Figure 10).

While there were no significant differences in in vitro antiproliferative activity against A549 among **10, 13** and *cis*-**14, 13** showed the most potent antitumor activity in vivo. In addition, **1** showing less potency in vitro than **10, 13** and *cis*-**14**, was as potent as **13** in vivo. The reason for the apparent discrepancy between the in vitro and in vivo data is not clear. However, considering that both **1** and **13** contain an aliphatic quaternary ammonium moiety like pyrrolidinium and piperidinium, the structural features might have an effect on pharmacokinetics such as distribution into xenograft tumors or retention in the body.

Conclusion

In conclusion, we synthesized a novel set of mono-adduct fullerene derivatives functionalized with pyridinium groups and found that they show potent antiproliferative activities against cancer cell lines including drug-resistant cells. Especially, **13** and *cis*-**14** have no stereoisomer and

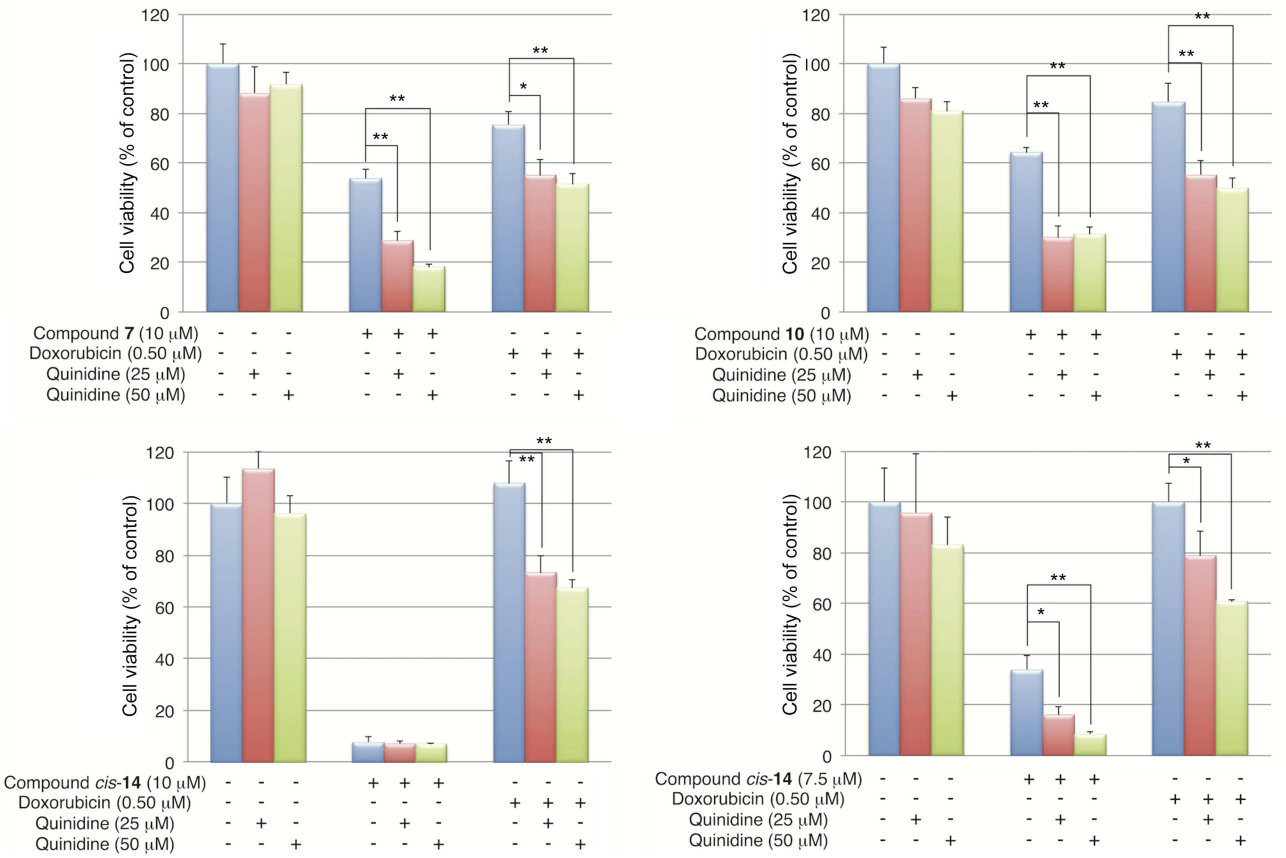

Figure 7 Effects of quinidine on fullerene derivatives-induced cell death in K562/ADM cells. Cells were co-incubated with quinidine and fullerene derivatives for 24 hrs. *$p<0.05$, **$p<0.01$.

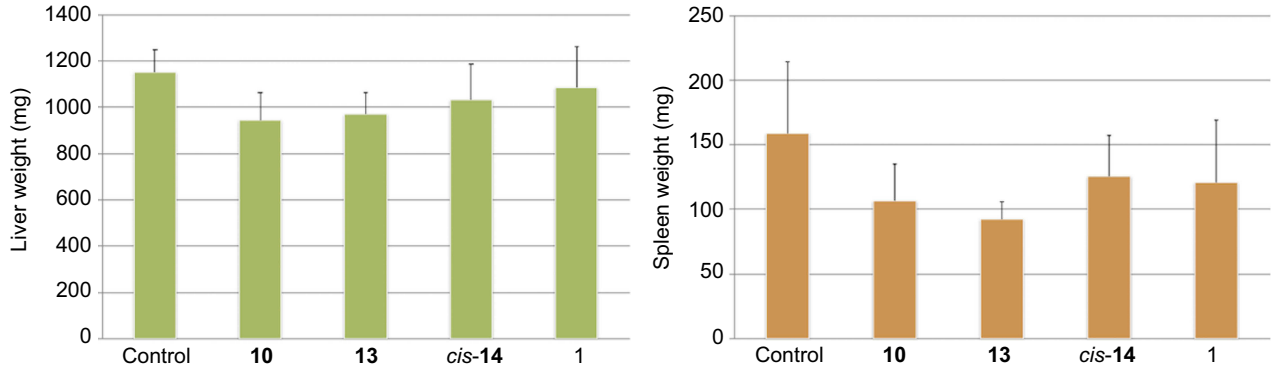

Figure 8 Weight of liver and spleen in A549-transplanted mice at Day 20. A549 cells (1.0×10^7 cells) were injected subcutaneously (s.c.) into female BALB/c nude mice aged 4 weeks. After injection of A549 cells, the mice were treated daily for 6 days with an intraperitoneal injection of fullerene derivatives. The animals were sacrificed and the weights of liver and spleen were recorded at two weeks after the last injection of fullerene derivatives.

strongly inhibited the proliferation of various cancer cell lines including drug-resistant cancer cell lines such as NIH:OVCAR-3 and K562/ADM, indicating that these fullerene derivatives newly synthesized in the present study have overwhelming superiority to **1** which has been evaluated in our previous research. Furthermore, these derivatives significantly suppressed the tumor growth in A549-transplanted mice without significant toxicity, proposing that they serve as the lead compounds for a novel type of antitumor agents.

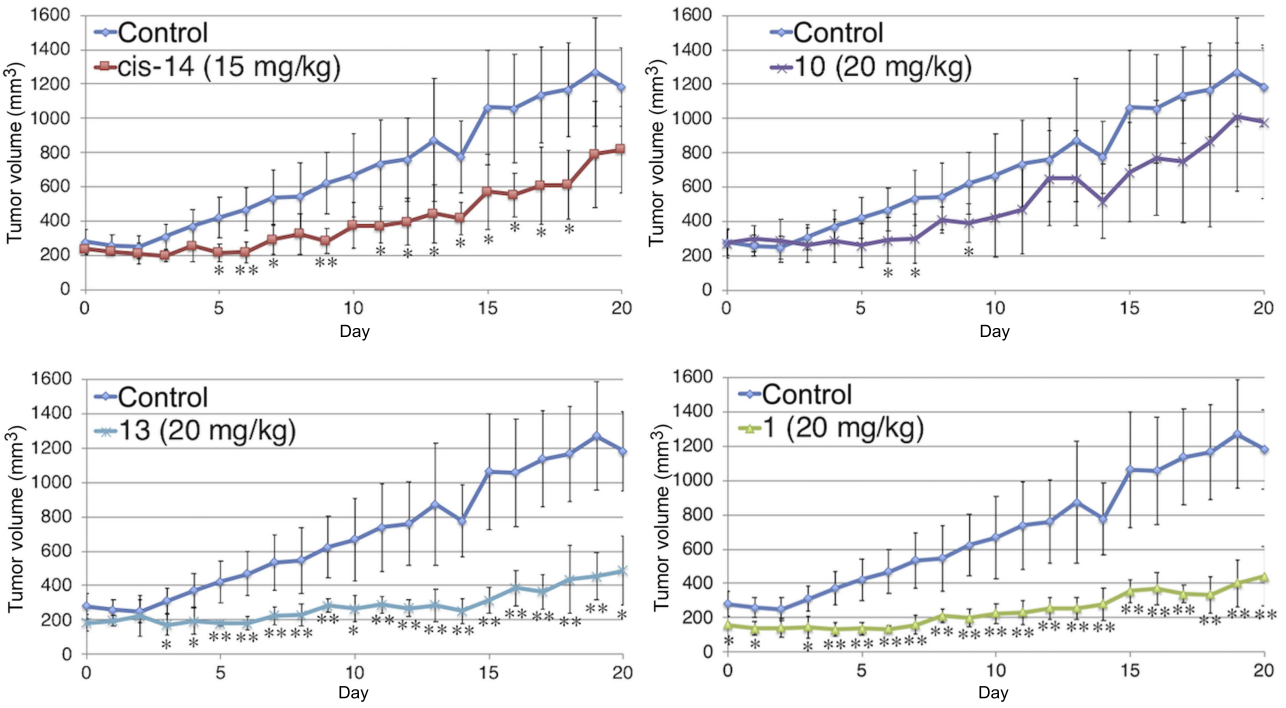

Figure 9 Time-dependent tumor growth in A549-transplanted mice from Day 0 to Day 20. After injection of A549 cells, the nude mice were treated daily for 6 days with an intraperitoneal injection of fullerene derivatives. The animals were sacrificed at two weeks after the last injection of fullerene derivatives. The tumor volume was determined with an electronic caliper once a day, the longer magnitude (L) and shorter magnitude (W) were measured and then converted into mg (mm^3) using $LW^2/2$. *p<0.05, **p<0.01, vs control *p<0.05, **p<0.01, VS control.

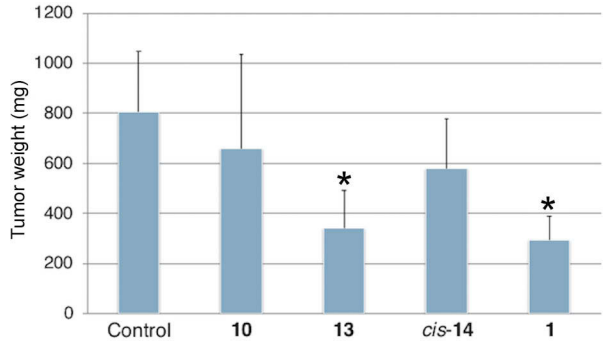

Figure 10 Tumor weight in A549-transplanted mice at Day 20. A549 cells (1.0×10^7 cells) were injected subcutaneously (s.c.) into female BALB/c nude mice aged 4 weeks. After injection of A549 cells, the mice were treated daily for 6 days with an intraperitoneal injection of fullerene derivatives. The animals were sacrificed and the tumor weights were recorded at two weeks after the last injection of fullerene derivatives. *p<0.05, VS control.

Abbreviations

MDR, multidrug resistant; P-gp, P-glycoprotein; SAR, structure activity relationship; DCFH-DA, 2',7'-dichlorodihydrofluorescein diacetate; ROS, reactive oxygen species; ADM, doxorubicin.

Acknowledgments

This work was supported by the Platform for Drug Discovery, Informatics, and Structural Life Science from the Ministry of Education, Culture, Sports, Science and Technology (MEXT) and by the Japan Agency for Medical Research and Development (AMED), 2012–2016, and the Platform Project for Supporting Drug Discovery and Life Science Research from AMED, 2017–2018.

Disclosure

The authors report no conflicts of interest in this work.

References

1. Narsimha S, Kumar NS, Battula KS, Nagavelli VR, Hussain SKA, Rao MS. Indole-2-carboxylic acid derived mono and bis 1,4-disubstituted 1,2,3-triazoles: synthesis, characterization and evaluation of anticancer, antibacterial, and DNA-cleavage activities. *Bioorg Med Chem Lett*. 2016;26(6):1639–1644. doi:10.1016/j.bmcl.2016.01.055
2. Eckford PDW, Sharom FJ. ABC efflux pump-based resistance to chemotherapy drugs. *Chemical Reviews*. 2009;109(7):2989–3011. doi:10.1021/cr9000226
3. Singh MS, Tammam SN, Shetab BMA, Lamprecht A. MDR in cancer: addressing the underlying cellular alterations with the use of nanocarriers. *Pharmacol Res*. 2017;126:2–30. doi:10.1016/j.phrs.2017.07.023
4. Kroto HW, Heath JR, O'Brien SC, Curl RF, Smalley RE. C_{60}:buckminsterfullerene. *Nature*. 1985;318:162–163. doi:10.1038/318162a0
5. Bosi S, Da Ros T, Spalluto G, Prato M. Fullerene derivatives: an attractive tool for biological applications. *Eur J Med Chem*. 2003;38(11–12):913–923.

6. Tokuyama H, Yamago S, Nakamura E, Shiraki T, Sugiura Y. Photoinduced biochemical activity of fullerene carboxylic acid. *J Am Chem Soc*. 1993;115(17):7918–7919. doi:10.1021/ja00070a064
7. Friedman SH, Ganapathi PS, Rubin Y, Kenyon GL. Optimizing the binding of fullerene inhibitors of the HIV-1 protease through predicted increases in hydrophobic desolvation. *J Med Chem*. 1998;41(13):2424–2429. doi:10.1021/jm970689r
8. Kataoka H, Ohe T, Takahashi K, Nakamura S, Mashino T. Novel fullerene derivatives as dual inhibitors of Hepatitis C virus NS5B polymerase and NS3/4A protease. *Bioorg Med Chem Lett*. 2016;26(19):4565–4567. doi:10.1016/j.bmcl.2016.08.086
9. Mashino T, Shimotohno K, Ikegami N, et al. Human immunodeficiency virus-reverse transcriptase inhibition and hepatitis C virus RNA-dependent RNA polymerase inhibition activities of fullerene derivatives. *Bioorg Med Chem Lett*. 2005;15(4):1107–1109. doi:10.1016/j.bmcl.2004.12.030
10. Nakamura S, Mashino T. Water-soluble fullerene derivatives for drug discovery. *J Nippon Med Sch*. 2012;79(4):248–254.
11. Yasuno T, Ohe T, Takahashi K, Nakamura S, Mashino T. The human immunodeficiency virus-reverse transcriptase inhibition activity of novel pyridine/pyridinium-type fullerene derivatives. *Bioorg Med Chem Lett*. 2015;25(16):3226–3229. doi:10.1016/j.bmcl.2015.05.086
12. Bosi S, Da Ros T, Castellano S, Banfi E, Prato M. Antimycobacterial activity of ionic fullerene derivatives. *Bioorg Med Chem Lett*. 2000;10(10):1043–1045.
13. Tsao N, Luh TY, Chou C, et al. In vitro action of carboxyfullerene. *J Antimicrob Chemother*. 2002;49(4):641–649. doi:10.1093/jac/49.4.641
14. Mashino T, Nishikawa D, Takahashi K, et al. Antibacterial and antiproliferative activity of cationic fullerene derivatives. *Bioorg Med Chem Lett*. 2003;13(24):4395–4397.
15. Nishizawa C, Hashimoto N, Yokoo S, et al. Pyrrolidinium-type fullerene derivatives-induced apoptosis by the generation of reactive oxygen species in HL-60 cells. *Free Radical Research*. 2009;43(12):1240–1247. doi:10.3109/13814780903260764
16. Yamori T. Panel of human cancer cell lines provides valuable database for drug discovery and bioinformatics. *Cancer Chemother Pharmacol*. 2003;52 Supp(1):S74–S79. doi:10.1007/s00280-003-0649-1
17. Filippone S, Maroto EE, Martín-Domenech Á, Suarez M, Martín N. Anefficient approach to chiral fullerene derivatives by catalytic enantioselective 1,3-dipolar cycloadditions. *Nat Chem*. 2009;1:578–582.